

## RESEARCH ARTICLE

# A requirement for p120-catenin in the metastasis of invasive ductal breast cancer

Sarah J. Kurley<sup>1</sup>, Verena Tischler<sup>2</sup>, Brian Bierie<sup>3</sup>, Sergey V. Novitskiy<sup>1</sup>, Aurelia Noske<sup>2</sup>, Zsuzsanna Varga<sup>2</sup>, Ursina Zürcher-Härdi<sup>2</sup>, Simone Brandt<sup>2</sup>, Robert H. Carnahan<sup>4,5</sup>, Rebecca S. Cook<sup>1</sup>, William J. Muller<sup>6,7</sup>, Ann Richmond<sup>1,8</sup> and Albert B. Reynolds<sup>1,8,\*</sup>

## ABSTRACT

We report here the effects of targeted p120-catenin (encoded by *CTNND1*; hereafter denoted p120) knockout (KO) in a PyMT mouse model of invasive ductal (mammary) cancer (IDC). Mosaic p120 ablation had little effect on primary tumor growth but caused significant pro-metastatic alterations in the tumor microenvironment, ultimately leading to a marked increase in the number and size of pulmonary metastases. Surprisingly, although early effects of p120-ablation included decreased cell–cell adhesion and increased invasiveness, cells lacking p120 were almost entirely unable to colonize distant metastatic sites *in vivo*. The relevance of this observation to human IDC was established by analysis of a large clinical dataset of 1126 IDCs. As reported by others, p120 downregulation in primary IDC predicted worse overall survival. However, as in the mice, distant metastases were almost invariably p120 positive, even in matched cases where the primary tumors were p120 negative. Collectively, our results demonstrate a strong positive role for p120 (and presumably E-cadherin) during metastatic colonization of distant sites. On the other hand, downregulation of p120 in the primary tumor enhanced metastatic dissemination indirectly via pro-metastatic conditioning of the tumor microenvironment.

**KEY WORDS:** p120 catenin, Breast metastasis, Colonization

## INTRODUCTION

Breast cancer is the second most common cause of cancer-related death in women. Although management of the disease has improved significantly over the past 10 years, metastasis remains a significant problem and the leading cause of mortality. Nonetheless, metastatic dissemination is a remarkably inefficient process (Valastyan and Weinberg, 2011). To successfully colonize distant sites in the body, cells from the primary tumor must acquire *de novo* the ability to (1) invade locally, (2) enter into circulation (intravasate), (3) exit from

circulation at a distant location (extravasate), and (4) thereafter survive as micrometastatic colonies in an otherwise hostile environment. Disseminated micrometastases are clinically undetectable and can remain dormant for years (Valastyan and Weinberg, 2011; Brabletz, 2012). The final and rate-limiting step in the metastatic cascade, termed colonization, occurs when micrometastatic lesions emerge from dormancy to form clinically relevant macrometastatic tumors.

Although many factors underlying these events are not well understood (Kang and Pantel, 2013), metastasis is frequently linked to genetic and/or epigenetic dysregulation of E-cadherin, the predominant cell–cell adhesion molecule in epithelial tissues and master organizer of the epithelial phenotype (Fan et al., 2019). As with other classical cadherins, its extracellular domains connect like cells via Ca<sup>2+</sup>-dependent homophilic interaction (Kim et al., 2011). Strong adhesion, however, is critically dependent on a group of cytoplasmic cadherin binding partners, namely  $\alpha$ -,  $\beta$ - and p120-catenins, each of which also contributes indispensably to the role of E-cadherin as a tumor suppressor (Jeanes et al., 2008; Schackmann et al., 2013b; Sun et al., 2014). Notably, direct interaction of E-cadherin with p120-catenin (encoded by *CTNND1*; hereafter denoted p120) is required for E-cadherin stability and retention on the cell surface. In many cell types, cadherin adhesion is compromised or lost altogether upon removal of p120, as the remaining components of the complex are then internalized by endocytosis and degraded (Thoreson et al., 2000; Ozawa, 2003; Wehrendt et al., 2016).

Consistent with these observations, experiments in mice based on targeted p120 ablation in various epithelial tissues have revealed potentially causal links to cancer in the salivary gland (Davis and Reynolds, 2006), esophagus (Stairs et al., 2011), skin (Perez-Moreno et al., 2008), pancreas (Hendley et al., 2016), intestine (Smalley-Freed et al., 2011) and breast (Kurley et al., 2012; Schackmann et al., 2013a; El Sharouni et al., 2017). *In vivo* p120-knockout (KO) phenotypes vary widely, however, depending on the organ (Perez-Moreno et al., 2006; Oas et al., 2010; Smalley-Freed et al., 2010), the degree of p120 depletion (Richert et al., 2005) and the context under which p120 depletion occurs (Mastracci et al., 2005; Macpherson et al., 2007; Short et al., 2017). During prostate maturation, for example, adhesion is largely unaffected by p120 KO despite near-complete loss of E-cadherin (Kurley et al., 2012). The developing mammary gland, on the other hand, is essentially disassembled, as epithelial adhesion is lost altogether (Kurley et al., 2012). Interestingly, tumorigenic effects of p120 ablation in the skin (Perez-Moreno et al., 2008) and the esophagus (Stairs et al., 2011) do not seem to be linked not to defective adhesion but rather a cell-autonomous inflammatory response (Perez-Moreno et al., 2006; Smalley-Freed et al., 2010; Stairs et al., 2011; Hu, 2012). By contrast, in adenomatous polyposis coli (*Apc*) mouse models of intestinal cancer, tumorigenesis was effectively blocked upon loss of both p120 alleles due to synthetic lethal interaction with the loss

<sup>1</sup>Department of Cancer Biology, Vanderbilt University, Nashville, TN 37232, USA.

<sup>2</sup>Institute of Surgical Pathology, University Hospital Zurich, Zurich, 8091, Switzerland.

<sup>3</sup>Whitehead Institute for Biomedical Research, Cambridge, MA 02142, USA.

<sup>4</sup>Department of Pediatrics, Vanderbilt University, Nashville, TN 37232, USA.


<sup>5</sup>Goodman Cancer Centre, Montreal, Quebec, H3A 1A3, Canada.

<sup>6</sup>Goodman Cancer Centre, Montreal, Quebec, H3A 1A3, Canada.

<sup>7</sup>Departments of Biochemistry and Medicine, McGill University, Montreal, Quebec, H3A 0G4, Canada.

<sup>8</sup>Vanderbilt-Ingram Cancer Center, Nashville, TN 37232, USA.

\*Author for correspondence (al.reynolds@vanderbilt.edu)

 S.J.K., 0000-0002-4127-1443; V.T., 0000-0002-6673-8329; B.B., 0000-0001-9367-9507; A.N., 0000-0002-0771-3180; Z.V., 0000-0001-6149-4225; U.Z., 0000-0002-6672-8104; S.B., 0000-0002-8558-6674; R.H.C., 0000-0001-5230-1532; W.J.M., 0000-0001-7690-0695; A.R., 0000-0002-9580-900X; A.B.R., 0000-0002-4514-0491

of *Apc* (Short et al., 2017). Loss of just one *p120* allele, on the other hand, resulted in up to a 10-fold increase in tumor multiplicity (Short et al., 2017). In mouse models of pancreatic cancer, monoallelic *p120* ablation was associated with metastasis to the liver while loss of both *p120* alleles led to pulmonary metastases (Reichert et al., 2018) revealing an unexpected dose-dependent effect of *p120* downregulation on metastatic organotropism.

In breast cancer (BC), specific subtypes have been selectively linked to altered levels of *p120* and/or E-cadherin. Inflammatory BC, for example, is associated with *p120* upregulation by an EIF4G and internal ribosome entry site (IRES)-mediated mechanism that leads to abnormally stable E-cadherin and the formation of highly metastatic tumor emboli (Silvera and Schneider, 2009; Silvera et al., 2009). In contrast, lobular BC is associated with complete loss of E-cadherin at a very early stage in its development (Berx et al., 1995; Vos et al., 1997; Singhai et al., 2011), a phenotype largely recapitulated by E-cadherin ablation in *p53* (also known as TP53) KO mice (Schackmann et al., 2013a; Derksen et al., 2011). With the loss of E-cadherin, *p120* mis-localizes to the cytoplasm, and metastases occur through a ROCK1-dependent mechanism (Schackmann et al., 2011). Interestingly, *p120* ablation in the same *p53* mutant mouse generates tumors that are E-cadherin-deficient and metastatic but do not recapitulate the lobular phenotype (Schackmann et al., 2013a; Hernández-Martínez et al., 2019). The effects of *p120*-ablation, therefore, are not necessarily the same as those caused by the loss of E-cadherin. Invasive ductal BC (IDC) is by far the most common BC subtype, accounting for ~80% of all human BC. Of note, *p120* downregulation occurs in over 50% of IDC (Sarrió et al., 2004) and has been linked to poor prognosis (Nakopoulou et al., 2002; Talvinen et al., 2010). Two small studies report regions of complete *p120* loss in ~10% of ductal carcinomas (Dillon et al., 1998; Nakopoulou et al., 2002). Nonetheless, the role of *p120* in the tumor progression and metastasis of IDC remains unclear.

Using MMTV-Cre; *p120*<sup>fl/fl</sup> mice, we showed previously that *p120* is essential for mammary gland development. Spontaneous Cre-mediated *p120* ablation at the onset of puberty (week 3) results in a pool of essentially non-adherent, E-cadherin-depleted cells that are lost altogether by week 6 (Kurley et al., 2012). In the present study, we crossed these mice onto an MMTV-PyMT background (i.e. MMTV-Cre; *p120*<sup>fl/fl</sup>; MMTV-PyMT) to examine the effect of *p120* ablation in the context of a well characterized *p53*-independent mouse model of IDC. Oncogenic transformation by PyMT rescued the *p120*-null population, which in spite of near complete loss of E- and P-cadherins, was then efficiently retained as *p120*-null and/or mosaic *p120*<sup>+/-</sup> primary tumors. The current study reports the outcome of these *p120*-ablation experiments on tumorigenesis and pulmonary metastasis.

## RESULTS

### Characterization of *p120* ablation in the MMTV-PyMT mouse model of breast cancer

To examine the role of *p120* in ductal breast cancer metastasis, we crossed our previously described mammary-specific *p120* knockout mouse (MMTV-Cre; *p120*<sup>fl/fl</sup>; Perez-Moreno et al., 2006; Kurley et al., 2012) to a well-characterized MMTV-PyMT mouse model of breast cancer (Lin et al., 2003). In the experimental cohort from this cross (MMTV-Cre; *p120*<sup>fl/fl</sup>; MMTV-PyMT), PyMT expression and *p120* ablation were induced simultaneously upon activation of the MMTV promoter at puberty (~3–4 weeks of age). We showed previously that in the absence of a transforming event, MMTV-Cre-induced *p120*-null cells were cleared from the developing gland and

lost altogether by the end of week 6, after which the gland was reconstituted normally from *p120*-retaining stem cells (Kurley et al., 2012). Here, we show that in the context of PyMT-induced transformation, *p120*-null cells are rescued and retained in primary tumors (Fig. 1A–C). Depending on the animal, the overall proportion of tumor cells lacking *p120* ranged from ~22–58% (mean of 38%) (Fig. 1B). *p120*-null regions of these primary tumors retained significant keratin-8 positivity (Fig. 1C), suggesting overall retention of epithelial identity. Surprisingly, mosaic *p120* ablation did not affect primary tumor latency or primary tumor volume (Fig. 1D,E), and differences in carcinoma cell apoptosis and proliferation were not statistically significant (Fig. S1A,B).

To assess the overall impact of *p120* ablation on the E-cadherin complex, we immuno-labeled *p120*-positive and -negative tumors with antibodies to E-cadherin and  $\beta$ -catenin (Fig. S1C,D). *p120* KO in mammary epithelium expressing the PyMT oncogene (mT) resulted in nearly complete loss of both E-cadherin and junctional  $\beta$ -catenin, as was previously observed in the absence of mT expression (Kurley et al., 2012). Loss of the E-cadherin complex occurs to varying degrees upon *p120* ablation as previously demonstrated in many epithelial tissues (Davis and Reynolds, 2006; Perez-Moreno et al., 2006; Stairs et al., 2011; Kurley et al., 2012), but the mammary gland is unusual in that E-cadherin staining is almost abolished upon *p120* KO.

MMTV-PyMT tumors typically display a mix of distinct morphological features during progression. In the absence of *p120*, we observed that hyperplastic *p120*-negative lesions contained epithelial cells with a more rounded morphology and increased intraluminal sloughing (Fig. S2A), apparently reflecting adhesion defects linked to E-cadherin loss. In addition, whereas late-stage MMTV-PyMT tumors typically contain a roughly even mix of pseudopapillary and characteristic adenocarcinoma phenotypes (Chetty and Serra, 2008), their *p120*-null counterparts were almost exclusively pseudopapillary (Fig. S2B).

### *p120* ablation blocks pulmonary metastatic colonization

To determine the effect of *p120* on pulmonary metastasis, we examined whole mounts of lungs from control and *p120* KO MMTV-PyMT animals that were collected 54 days following initial tumor palpation (Fig. 2). Notably, metastatic lesions in the *p120* KO model were substantially larger (Fig. 2A; quantified in 2C) and 4-fold more numerous (median of 3 in controls compared to 12.5 in KOs) (Fig. 2B) than those from *p120*-positive controls, revealing a strong, apparently pro-metastatic, impact of *p120* ablation. Surprisingly, however, immunolabeling experiments revealed that the actual pulmonary metastases from *p120*-KO animals were predominantly *p120* positive (Fig. 2D,E). Examples of the *p120* content of individual pulmonary metastases from these animals are shown in Fig. 2D (i.e. positive, mixed and negative). To document the overall distribution of *p120* positivity, metastases were scored as entirely positive, mostly positive, mostly negative or entirely negative, and then quantified in each of six randomly selected *p120* KO mice (Fig. 2E).

Of note, entirely *p120*-negative metastases were exceedingly rare. They manifested in one animal only (mouse #6) and comprised only 15% of the total number of lung metastases in that animal (as opposed to 70% entirely positive). By contrast, in two animals (numbers 4 and 5), all of the metastases were entirely *p120* positive. Moreover, irrespective of the mix, metastases in all six animals demonstrated strong selection for *p120* positivity. These data suggest that despite the pro-metastatic effects of *p120* ablation in primary tumors, retention of *p120* confers a strong selective advantage with respect to establishing distant metastases.

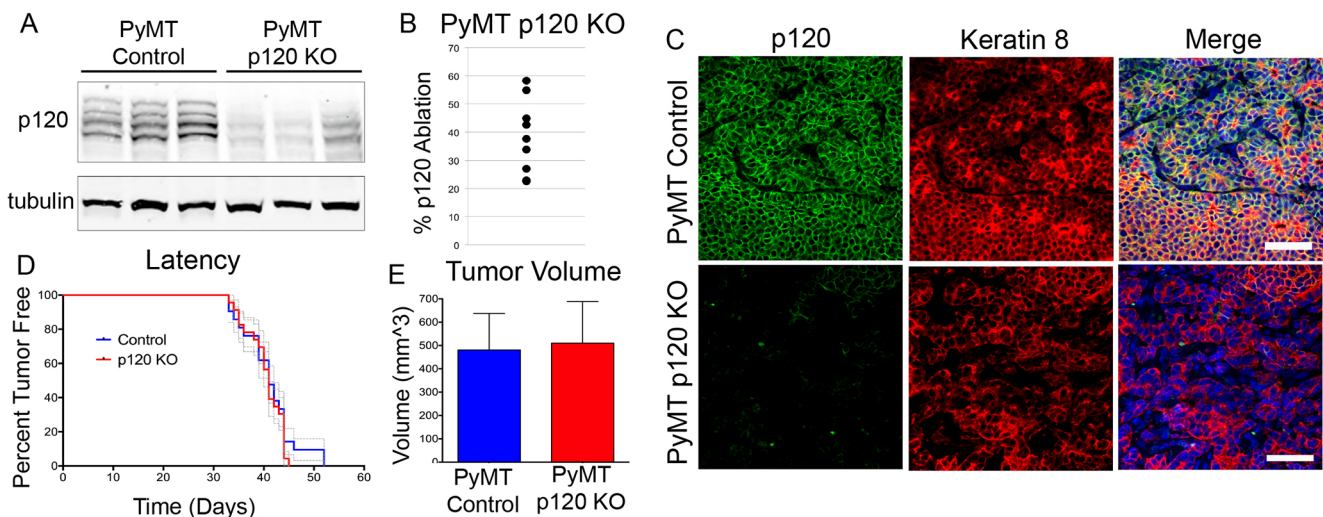


**Fig. 1. Latency and tumor volume are not altered by mosaic ablation of p120 in PyMT-induced mammary tumors.** (A–C) Characterization of p120 status in tumors from control (MMTV-PyMT; MMTV-Cre) and p120 KO (MMTV-PyMT; MMTV-Cre; p120<sup>fl/fl</sup>) mice. The p120 KO MMTV-PyMT p120 status in knockout and control mice was assessed by western blotting (A) and immunofluorescence (C). The proportion p120 KO cells in primary mammary tumors was estimated by p120 immunofluorescence staining of tumors from eight MMTV-Cre; p120<sup>fl/fl</sup>; MMTV-PyMT mice euthanized 54 days post palpation (B). Each point represents the percentage of carcinoma cells exhibiting p120 ablation averaged across three sections of random tumor sample per mouse. Scale bars: 50  $\mu$ m. (D) Control and p120-ablated mice were monitored for tumors by palpation ( $n=21$  WT, blue;  $n=23$  p120 KO, red). This  $n$  of >20 gives sufficient power ( $\sim 90\%$ ) to detect significant differences. No difference in latency was observed using a log-rank test. (E) The volumes of all ten mammary tumors per mouse were approximated by caliper ( $h \times l \times w = \text{approx. volume}$ ) at 54 days post palpation. Mean  $\pm$  s.d. volumes per mouse are shown ( $n=6$  WT blue,  $n=5$  p120KO red). No significant difference was observed using a Mann–Whitney test.

To identify particular events in the process that might account for this enrichment, we used Cre recombinase-based methods to generate matched sets of polyclonal and monoclonal p120-positive (wild type, WT) and p120-negative (KO) PyMT tumor

cell lines (Fig. 3). As shown above *in vivo* (Fig. 1; Fig. S1), p120-null cells displayed near-absent levels of E-cadherin, but retained expression of the epithelial marker keratin-8 (Fig. 3A), suggesting retention of epithelial identity. Note that among the p120-null cell

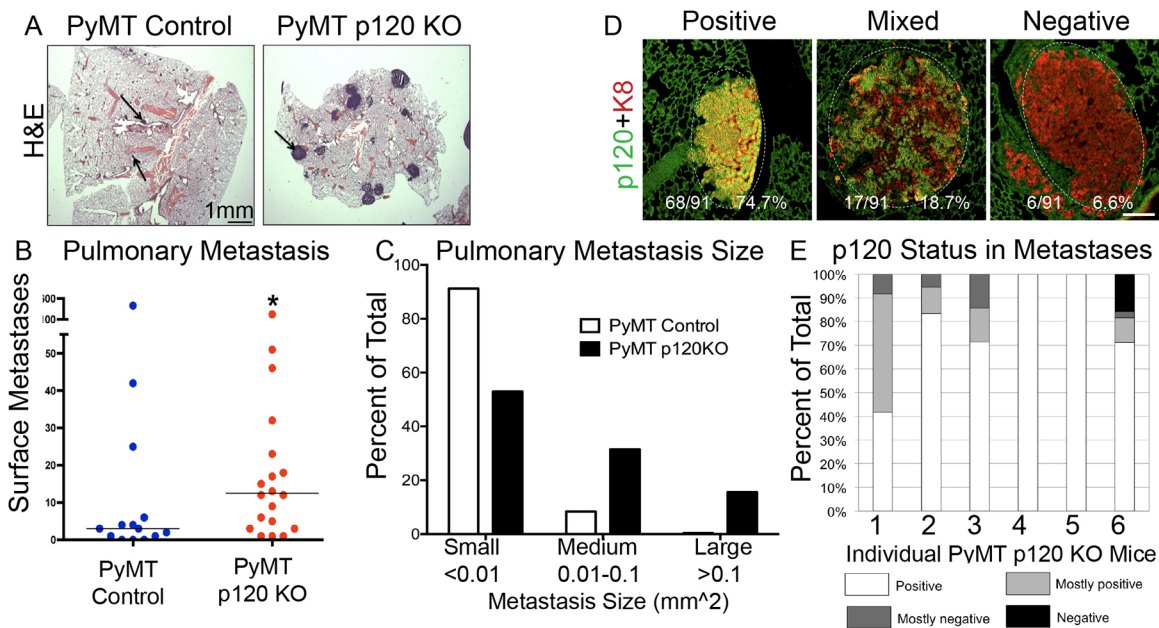


**Fig. 2. Primary tumor p120 ablation increases quantity and size of pulmonary metastases while selecting against p120-null cells.** (A) Representative metastasis size is shown in lung sections stained with H&E. Scale bar: 1 mm. (B) Visible (surface) lung metastases were quantified by Hematoxylin staining performed on cleared lung whole mounts removed 54 days post tumor palpation. The mean is indicated.  $*P < 0.05$  (Mann–Whitney test). (C) Mean metastasis size was of lung sections stained with H&E and binned into the described sizes;  $n=8$  PyMT Control and  $n=12$  PyMT p120KO mouse lungs. (D,E) Lungs from PyMT p120 KO mice were stained for p120 and keratin 8 and analyzed through immunofluorescence. After identification of PyMT cells by keratin 8 positivity, lung metastases were analyzed for p120 status. (D) Representative examples of pulmonary metastases (outlined by a dashed line) stained for p120 and keratin 8. Collective binning data from 91 metastases from 6 PyMT p120 KO mice are shown. Scale bar: 2 mm. (E) All visible metastases from  $n=6$  PyMT p120 KO mice were assessed and binned into positive (white), mostly positive (light gray), mostly negative (dark gray) and negative (black). Data shown by each individual mouse.

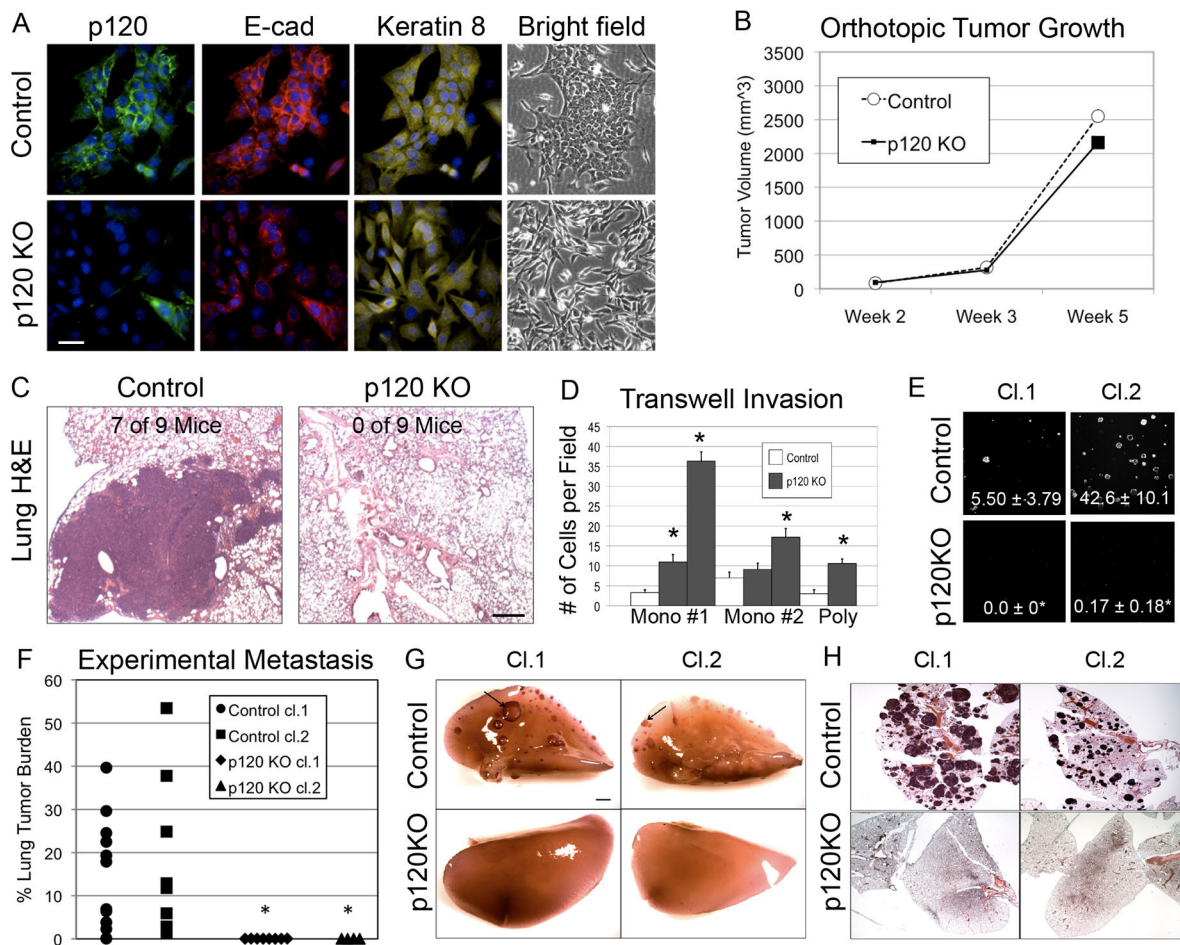


**Fig. 3. p120 ablation induces invasion but blocks pulmonary colonization.** Cell lines were generated from MMTV-PyMT; p120<sup>fl/fl</sup> mice and were infected with empty or Cre-expressing retrovirus to generate control or KO cells. (A) Co-immunofluorescence for p120, E-cadherin and keratin-8 confirms a predominantly p120-negative and keratin-8-positive polyclonal population. KO cells are fibroblastic on plastic compared to the cobblestone, epithelial control cells as evidenced by bright field imaging. Scale bar: 200  $\mu$ m. (B)  $10^6$  polyclonal cells expressing empty or Cre-recombinase vector were injected into an orthotopic site. Tumor growth of control and p120 KO cells transplanted into the orthotopic site of nude mice was monitored by calipers. Results are representative of 2 repeated experiments. (C) After 5 weeks, pulmonary metastases were assessed by H&E staining of lung sections. Control cells, but not KO cells metastasize to the lungs when transplanted into mammary glands of nude mice. Representative H&E-stained sections of pulmonary tissue are shown above. The arrow denotes a metastasis. Scale bar: 2 mm. (D) *In vitro* invasion assays were performed using three independently derived PyMT cell lines (two monoclonal and one polyclonal) infected with control or Cre lentivirus. Ten random fields of view per transwell were assessed after 36 h. Assays were performed two independent times and a representative graph (mean  $\pm$  s.d.) is shown. \* $P < 0.001$  (Student's *t*-test). (E) PyMT-derived cell lines were grown in agar for 3.5 weeks. Representative images at 2.5 $\times$  magnification are shown. Quantification of growth in soft agar from two independent experiments is represented as mean  $\pm$  s.d. number of colonies per full field. \* $P < 0.01$  (Student's *t*-test for KO compared to either control). (F–H) PyMT-derived cells were injected into the tail veins of female mice and assayed for lung tumor burden after 4 weeks. (F) Quantification of tumor burden in H&E stained sections. \* $P < 0.01$  (Mann–Whitney). Representative lung-whole mount images (G) and H&E stained lung sections (H) are shown. Scale bar: 1 mm (in G for G,H). Arrows in G denote metastases.

lines isolated from individual tumors, there were occasional p120-positive cells that served as internal positive controls (e.g. Fig. 3A, lower left panel). Interestingly, p120 KO induced superficial characteristics of mesenchymal cells (Fig. 3A, bright field panels), raising the possibility of a bone fide epithelial–mesenchymal transition (EMT). On the other hand, loss of intercellular adhesion following p120 ablation would be expected to phenocopy many of the effects of EMT. Although not necessarily definitive, we observed that mRNAs typically upregulated by classical EMT [e.g. vimentin, snail (also known as *Snai1*), slug (*Snai2*), Zeb1, Sma (also known as *Acta2*) and S1004A] were not upregulated in a microarray dataset derived from p120 KO PyMT cells (data not shown). The simplest interpretation of these data, therefore, is that the mesenchymal-like phenotype observed is instead due to adhesive defects caused by p120 ablation.

*In vivo* effects of p120 ablation on tumor initiation and progression were assayed by transplanting isogenic p120-positive and -negative PyMT cell lines into the cleared mammary fat pads of WT recipients. Similar to the results observed in the autochthonous mouse models, primary tumor latency and growth were not significantly affected by the absence of p120 (Fig. 3B). However, lung metastases were evident in 77.8% of mice transplanted with p120-positive tumor cells, whereas metastases were virtually absent from mice transplanted with the isogenic p120-null counterparts (Fig. 3C). Thus, p120 KO in this model had relatively minor effects at the level of the primary tumor but almost completely blocked the formation of distant metastases.

To identify which stage(s) of the metastatic cascade were impaired by p120 loss, we assayed several metastasis-associated parameters, comparing MMTV-PyMT-transformed cell lines (controls) to their p120 KO counterparts. Cell motility was examined by an *in vitro*

wound-healing assay. In the presence of p120, 'wounded' cell monolayers were closed primarily by a process of collective migration. By contrast, p120 KO cells exhibited primarily single-cell migration, which was only marginally less efficient (e.g. see movie in Kurley et al., 2012). *In vitro* invasion assays, on the other hand, showed that p120 KO cells were 2–10-fold more efficient at penetrating transwell filters coated with Matrigel, a model extracellular matrix (Fig. 3D). Intravasation and survival in the bloodstream is typically assayed by quantification of circulating tumor cells in blood. However, for reasons that are unclear, the method is notoriously difficult to reproduce in MMTV-PyMT mouse models (Muraoka et al., 2002). Although we found no statistical difference in the results from control and p120-ablated animals, the number of cells isolated were typically low and highly variable in both cohorts (Fig. S3A,B). Taken together, however, these data suggest that p120-ablation enhances several mesenchymal cellular characteristics, including fibroblast-like morphology, a transition from collective to single-cell migration, and a marked increase in invasive behavior, alterations likely to be pro-metastatic with respect to the early steps in the metastatic cascade.

As mentioned above, generally acknowledged properties associated with metastatic capacity include the ability to (1) intravasate, (2) survive in the bloodstream, (3) extravasate, and/or (4) survive and proliferate post-extravasation in effectively hostile foreign microenvironments. To further examine the ability of cells to survive in circulation and subsequently extravasate, isogenic p120-positive or -negative PyMT tumor cells were labeled with a fluorescent dye and injected directly into circulation via the tail vein. Intraluminal survival/extravasation and subsequent clearance from the lungs were monitored by fluorescence microscopy at 1- and 6-h time points, respectively (Fig. S3C). p120 ablation, however, did not affect the number of cells retained in the lung at either time point, suggesting that p120 KO does not substantially alter the kinetics of extravasation and/or the subsequent clearance from the lung.

In the metastatic cascade, progression from disseminated micrometastases to clinically relevant macrometastatic lesions, is referred to as metastatic colonization. We postulated that p120 might be essential for (1) formation/survival of micrometastatic lesions, or alternatively, (2) for the outgrowth of established micrometastases into macroscopic secondary tumors. To test the hypothesis, isogenic p120-positive or -negative PyMT cell lines were injected through the tail vein and animals were assayed 21 days later for metastatic colonization of the lung (Fig. 3F–H). Remarkably, WT PyMT-transformed cells (i.e. p120 positive) formed large numbers of macrometastatic lesions while their isogenic p120 KO counterparts were completely deficient in this process.

To clarify the underlying mechanism(s), we conducted soft agar colony formation assays to determine whether p120 KO cells were capable of anchorage-independent cell growth, an *in vitro* surrogate for tumorigenicity. We found that p120 ablation eliminated an otherwise robust ability of WT PyMT cells to undergo anchorage-independent cell growth. Thus, p120 loss in PyMT-transformed cells confers a cell-intrinsic anchorage-independent growth defect that may be related to its *in vivo* defect in pulmonary colonization (Fig. 3E).

### **p120-dependent regulation of the primary tumor microenvironment**

Paradoxically, although p120 ablation markedly increased the size and number of pulmonary metastases, the actual metastatic lesions were almost invariably p120 positive. A potential explanation is that the p120-ablated component of primary PyMT tumors might

indirectly promote a significant pro-metastatic microenvironment. For example, p120 ablation in some tissues (e.g. skin and esophagus) leads to cell-autonomous inflammation, which has been causally linked to tumorigenesis (Perez-Moreno et al., 2008; Stairs et al., 2011). Thus, we interrogated the primary tumor microenvironments from cohorts of PyMT and PyMT/p120 KO mice (Fig. 4). Notably, significantly increased abundance of macrophages (F4/80 positive) and myofibroblasts (SMA positive) were observed in regions of p120 ablation (Fig. 4A,B, respectively). Trichrome Blue staining indicated higher levels of collagen deposition in the p120-null tumors (Fig. 4C). Other cell populations within the primary tumor microenvironment, including several types of vasculature and CD3<sup>+</sup> T-cells, were consistent between the two models (Fig. S5A–C). Overall, these data illustrate that there are distinct alterations in the tumor stroma associated with p120-ablated epithelium.

To further characterize the primary tumor microenvironment, we analyzed macrophage infiltration and phenotype by flow cytometry and quantitative real-time RT-PCR (qRT-PCR). To quantify macrophage recruitment, tumors were dissociated and viable cells were analyzed by flow cytometry using antibodies that collectively detect macrophages (CD45<sup>+</sup>, CD11b<sup>+</sup> and F4/80<sup>+</sup>). By this method, we determined that total macrophage numbers were unaltered in PyMT p120-KO mice (data not shown). Thus, F4/80-positive macrophage populations observed in Fig. 2A may reflect locally enhanced recruitment to regions of p120 ablation, as opposed to the whole tumor. Macrophages exist in a variety of phenotypic states, including anti-tumor M1 and pro-tumor/pro-metastasis M2 states (DeNardo and Coussens, 2007). By performing flow cytometry using well-established M1 and M2 markers, we determined that the proportion of M1-like tumor macrophages were similar in p120 WT and p120 KO samples. However, M2 macrophages, were significantly increased in p120 KO tumors (Fig. 4D), suggesting a pro-tumor and/or pro-metastasis bias. To assess transcript levels, RNA from flow-sorted populations of CD45<sup>+</sup> CD11b<sup>+</sup> F4/80<sup>+</sup> tumor macrophages was assessed by qRT-PCR analyses. Results from this analysis revealed significantly increased *Mmp2* and *Mmp9* (M2-like markers), and decreased M1-like markers *Tnf* and *Il12b* (Fig. 4E), confirming a shift in tumor macrophage phenotypes that is consistent with pro-metastatic progression. Therefore, we postulated that p120-ablated tumor cells might selectively secrete factors known to function in the recruitment of macrophages. Conditioned medium from p120-negative PyMT cells was 3- to 10-fold more effective in the *in vitro* recruitment of peritoneal macrophages than medium from control (p120-positive) cells (Fig. 4F). Thus, p120 ablation in the context of PyMT-expressing mammary tumor cells elicits secretion of as-yet-unidentified factors that may account for the activities of p120-negative PyMT cells in the recruitment and/or behavior of resident macrophage populations.

### **Reduced p120 in primary tumors associates with a less-favorable outcome**

p120 levels are frequently reduced and sometimes lost altogether in a wide variety of epithelial cancer types, including BC (Thoreson et al., 2000). To clarify inconsistencies in the pathology literature on ductal breast cancer, p120 expression was examined by immunohistochemistry in a cohort of 1126 patients with primary invasive ductal breast cancer. Details of the patient cohort are provided in Table S1. Fig. 5A shows representative examples of p120 expression in invasive ductal breast cancer corresponding to IHC scores 0–3 (top 4 panels, as indicated in lower left corner of each), as compared to normal breast (first panel in row 3) and ductal carcinoma *in situ* (DCIS) stained for p63 (row 3, first half of second panel, as

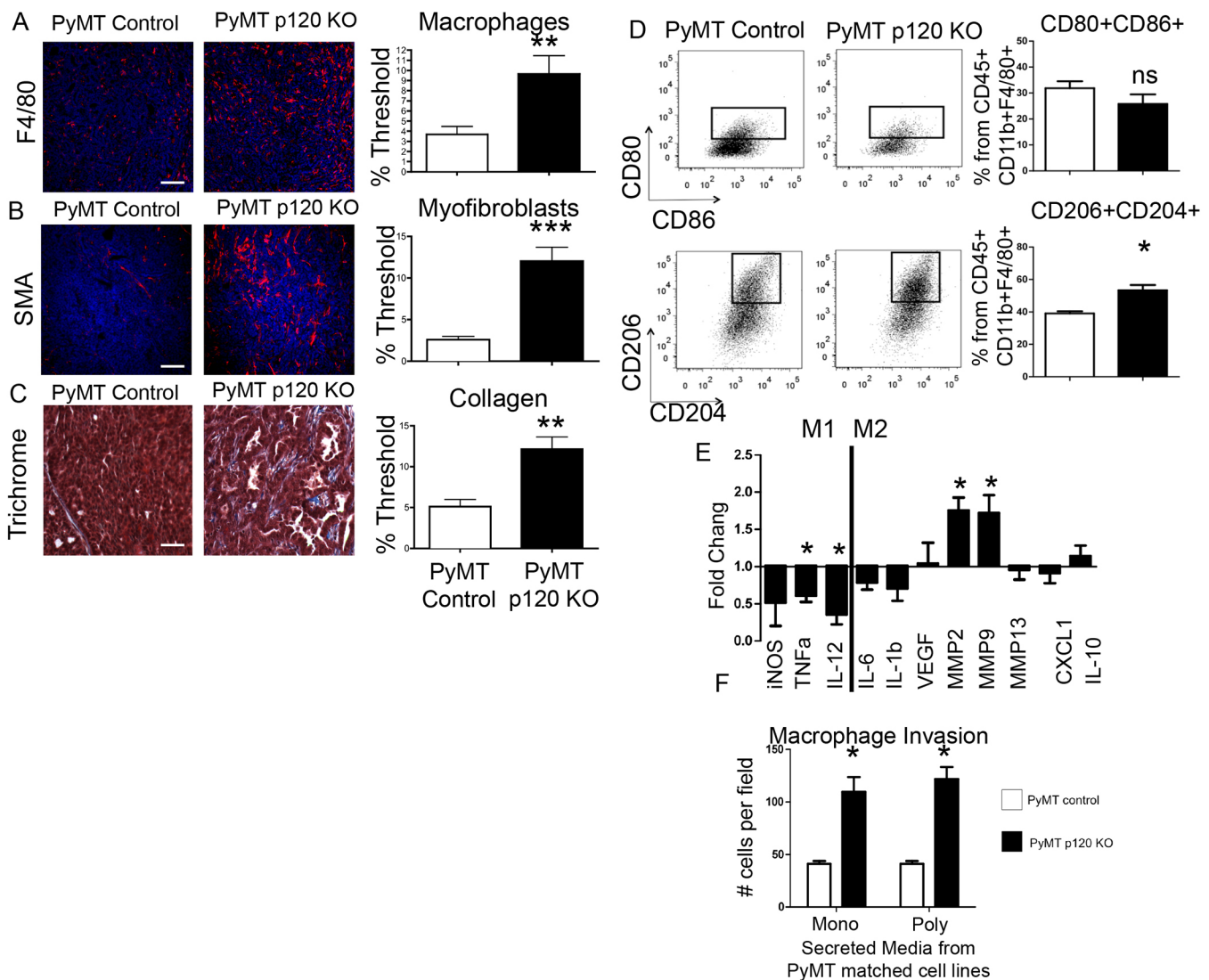


**Fig. 4. p120 ablation induces infiltration of M2 macrophages.** (A–C) PyMT tumor sections were immuno-stained for F4/80 (A) or SMA (B) to detect macrophages and myofibroblasts, respectively. Nuclei are stained with Hoechst dye. To detect collagen, sections were stained with trichrome blue (C). Scale bars: 200  $\mu$ m. Graphs to the right quantify these factors directly by the indicated measurements, and are mean  $\pm$  s.d.;  $n=6$  mice per genotype with six random 20 $\times$  images per single section were assessed. White bars are PyMT Control and black bars are PyMT p120 KO. Three regions of random tumor sample per mouse were assayed ( $n=5$  per genotype). \*\* $P<0.01$ , \*\*\* $P<0.0001$  (Mann–Whitney test). (D) Flow cytometry analysis of CD45<sup>+</sup> CD11b<sup>+</sup> F4/80<sup>+</sup> cells in tumor tissue for cell surface markers of M1 (top, CD80<sup>+</sup> CD86<sup>+</sup>) and M2 (bottom, CD206<sup>+</sup> CD204<sup>+</sup>) phenotype. Representative FACS plots of macrophage numbers in tumor tissue. Plots are gated as CD45<sup>+</sup> DAPI<sup>-</sup>. Plots depict mean  $\pm$  s.e.m.,  $n=5$  mice per group. \* $P<0.05$ ; ns  $P>0.05$  (Mann–Whitney). (E) qRT-PCR on CD45<sup>+</sup> CD11b<sup>+</sup> F4/80<sup>+</sup> cells from PyMT Control and PyMT p120 KO tumor tissues sorted by FACS Aria and converted to cDNA. Data are shown as fold over control. (F) Macrophage invasion assay. Monoclonal or polyclonal-matched PyMT-derived cell lines were grown in 3D cultures. After establishment of colonies, serum-free medium was added and collected after 24 h. Peritoneal macrophages were derived and plated onto Matrigel-coated transwells. Macrophages were allowed to invade for 48 h toward control or p120 KO cell secreted medium. This graph is mean  $\pm$  s.d. representative of two replicates; 10 fields per transwell were assessed for number of cells per field. \* $P<0.05$  (Student's  $t$ -test).

labeled) or p120 (row 3, second half of second panel, as labeled). High p120 expression (score 3) was observed in 49.7% of the primary tumor samples, similar to p120 staining intensity seen in normal breast (score 3) (Fig. 5A; Table S1). Complete loss of p120 (e.g. Fig. 5A, row 1, first panel) was observed in 7.5% of the cases.

Partial p120 loss (scores 1 and 2) and complete p120 loss (score=0) correlated with higher tumor grade, higher primary tumor (pT) stage and estrogen receptor negativity (Table S1). We found no correlations with other parameters such as nodal stage and *HER2* status, and nearly all DCIS cases (128/129, 99.2%) showed strong (score=3) p120 expression (e.g. Fig. 5A, row 2, second panel). Staining for p120 was localized primarily to plasma membranes, and cytoplasmic

p120 expression was observed in only 96/1126 cases (8.5%), consistent with previously published data on ductal breast cancer (Sarrío et al., 2004).

Overall, statistical analyses show that reduced or absent p120 in primary invasive ductal breast cancer is significantly associated with a worse outcome (Fig. 5B). By multivariate analysis, p120 did not qualify as an independent prognostic factor [compared with pT, grade, patient normal (pN) and with/without estrogen receptor]. However, patients with complete or partial loss of membranous p120 expression had significantly shortened overall survival in a univariate analysis ( $P=0.027$ ) (Fig. 5B). In addition, patients whose tumors showed complete

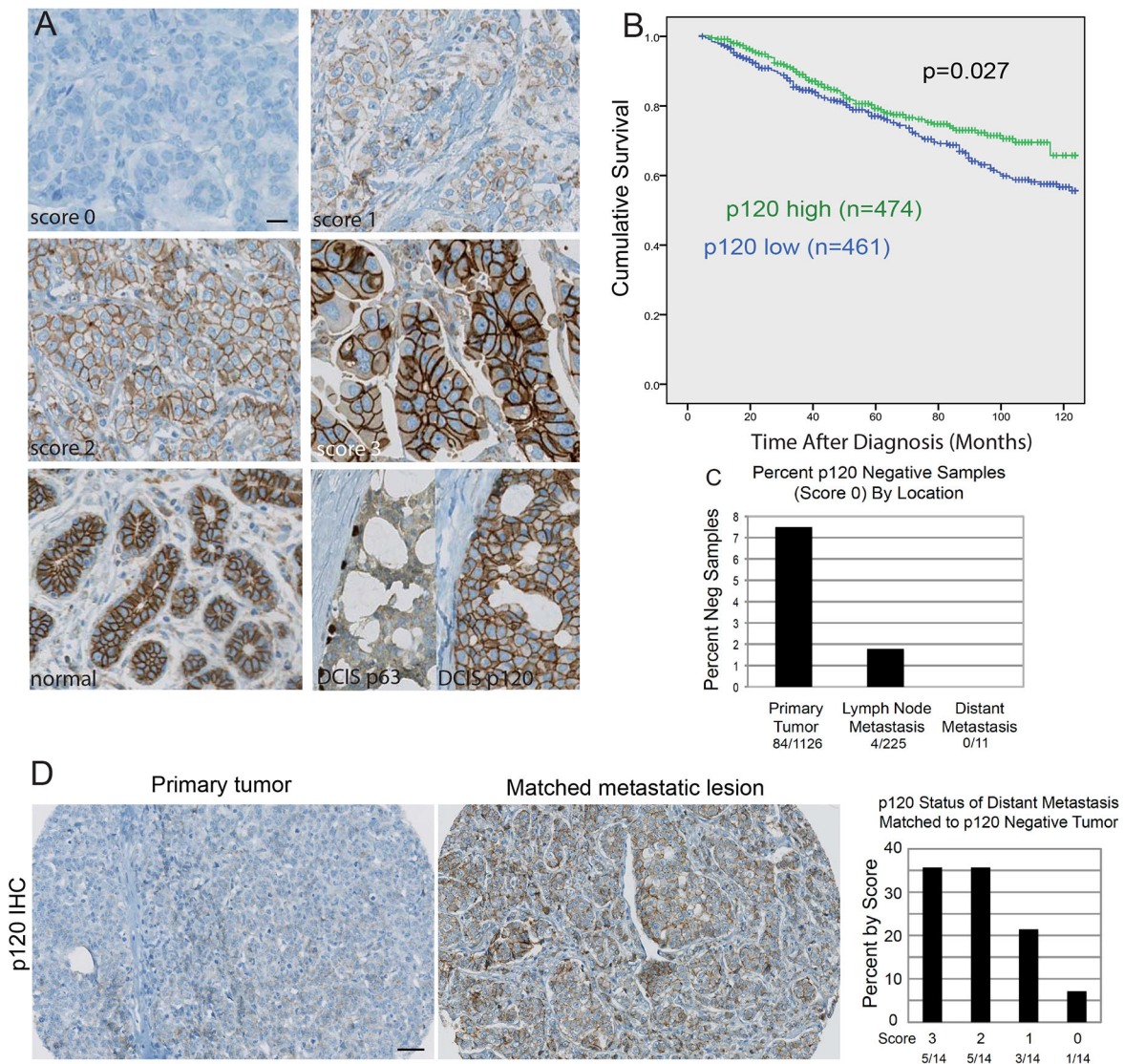


**Fig. 5. p120 expression in invasive breast cancer metastasis.** (A) Representative examples of p120 expression in invasive ductal breast cancer (scores 0–3), normal breast glands (row 3 first panel) and DCIS (row 3, second panel: p63 staining for myoepithelial cells) using IHC. Scale bar: 100  $\mu$ m. (B) A Kaplan–Meier curve illustrating that there is a significantly shorter overall survival (censored at 120 months) for the patient group with altered p120 expression ('p120 low' scores 0–2) compared to 'p120 high' expression (score 3),  $P=0.027$ . (C) Distribution of p120 negative samples by location of source tissue. (D) Representative IHC images of p120 negative samples ( $n=14$ ) and matched metastatic disease. Scale bar: 500  $\mu$ m. Graph denotes distribution of p120 status in matched metastases of p120 negative primary tumors.

p120 loss (score 0,  $n=73$ ) versus all other levels (score 1–3,  $n=862$ ) at the time of histology had a significantly shorter overall survival ( $P=0.011$ ).

#### p120 loss in distant and/or lymph node metastases is rare

Extending the analysis to breast cancer metastatic lesions, we initially examined p120 in 225 lymph node and 11 distant (non-lymph node) metastases. Immunohistochemistry for p120 in lymph node metastases ( $n=225$ ) indicated strong expression in 48.9% of cases (110/225) (score 3), reduced expression in 36.9% of cases (83/225) (score 2), weak expression in 12.4% of cases (28/225) (score 1) and absent p120 staining in 1.8% of cases (4/225). In the set of distant (non-lymph node) metastases ( $n=11$ ), p120 was expressed in 100% of cases (45.5% scored 1 or 2, 54.5% scored 3) (Fig. 5C).

Next, we interrogated a set of metastases from individuals whose primary tumors were p120 negative. Of the 84 primary invasive ductal breast cancer cases with complete loss of membranous p120

staining, 14 cases of matched metastatic disease (16.7%) were available from the archives. Of these, 5/14 (35.7%) expressed high levels of p120 (score 3), 5/14 (35.7%) showed reduced levels (score=2), 3/14 (21.5%) scored weakly (score=1) and one (7.1%) was negative (score=0) (Fig. 5D). Thus, despite complete absence of p120 staining in all 14 primary tumors, all but one of the metastases were p120 positive, and the majority (10/14) were either normal (5/14, score 3) or moderately reduced (5/14, score 2).

#### DISCUSSION

The vast majority of human BC (~80%) manifests as IDC, as modeled here in MMTV-PyMT mice. Downregulation of p120 in IDC is associated with poor prognosis (Saijo et al., 2001; Wijnhoven et al., 2005), but underlying mechanism(s) are not well understood. Importantly, we found that pulmonary metastases obtained from human IDC patients were almost invariably positive for p120, even in matched samples where the primary tumors were

p120 negative. This seeming contradiction is addressed in the current study using mouse models for insight into mechanism and human IDC samples to validate our observations in mice.

We previously demonstrated that MMTV-targeted p120 ablation during development of the mammary gland resulted in completely non-adherent cells that were unable to participate in formation of the gland. By 6 weeks, this non-adherent pool was lost altogether and replaced by normal mammary tissue reconstituted from a residual pool of p120-retaining stem cells (Kurley et al., 2012). In the current study, we used the MMTV-mT mouse model to directly examine the effects of mosaic p120 ablation in the context of a transforming oncogene. Indeed, transformation by PyMT rescued the viability of a p120-negative pool that otherwise did not survive. Unexpectedly, however, the absence of p120 did not exacerbate metastasis, but rather suppressed the strong metastatic proficiency normally conferred by PyMT.

Collectively, our results suggest a strong selective pressure for retention of p120 during metastatic colonization of distant sites. To validate this hypothesis experimentally, we generated isogenic mT-transformed cell lines differing only by the presence or absence of p120. Notably, in orthotopic implantation experiments, the absence of p120 had little impact on primary tumor latency or volume, as observed initially in the autochthonous model, but metastasis was abolished. This effect was particularly striking when assayed by tail vein injection (i.e. lung colonization assays), a procedure that bypasses the primary tumor altogether to pinpoint activities that are selectively relevant to the colonization of distant sites. Remarkably, p120-ablated cell lines exhibited no evidence of colonization, whereas their p120-expressing parental counterparts were aggressively metastatic. Consistent with these data, p120 ablation also eliminated an otherwise robust ability of these cells to undergo anchorage-independent cell growth. Thus, expression of p120 in these mT-transformed cell lines is apparently required for anchorage-independent growth, and importantly, for distant metastatic colonization.

This requirement for p120 during metastatic colonization is most likely explained by its essential role in maintaining E-cadherin stability. Despite the reputation of E-cadherin as a potent metastasis suppressor, compelling evidence suggests that several modes of metastatic dissemination and/or colonization may actually depend on the expression or re-expression of E-cadherin. In general, models to this effect fall into one of two main categories. The first invokes metastatic dissemination by collective migration (Huang et al., 2015; VanderVorst et al., 2019; Cheung and Ewald, 2016), a process known to require p120 and its stabilizing effect on E-cadherin (Macpherson et al., 2007; Kota et al., 2019; Gritsenko et al., 2020). The second invokes dissemination via EMT, which confers a spectrum of mesenchymal traits that enable and/or promote metastatic behavior (e.g. exchange of E-cadherin for N-cadherin, mesenchymal cell morphology, invasive behavior, cancer stem cell properties and anchorage independence) (Jones et al., 2014; Hernández-Martínez et al., 2019). Importantly, EMT is reversible, and several lines of evidence suggest that successful metastatic colonization following dissemination by EMT depends ultimately on the reversal of this process (i.e. mesenchymal-to-epithelial transition; MET), as evidenced in part by frequent re-expression of E-cadherin in distant metastatic lesions (i.e. MET) (Wells et al., 2008; Brabletz, 2012; Gunasinghe et al., 2012). A third model suggested recently by Ewald and colleagues poses an essential role for E-cadherin as a survival factor (Padmanaban et al., 2019). In the absence of E-cadherin, increased TGF $\beta$ 3 signaling leads to elevated levels of reactive oxygen species and an apoptotic

response to conditions imposed by the metastatic cascade. Notably, all of these models ultimately posit essential roles for E-cadherin that are p120-dependent.

A hallmark of classic EMT (and partial manifestations thereof) is the upregulation of a mesenchymal cadherin (usually N-cadherin) at the expense of E-cadherin, whose expression is simultaneously reduced or lost altogether. The mesenchymal properties of N-cadherin are closely associated with increased cell motility, invasion and other aspects of metastatic dissemination (Thiery et al., 1988; Gritsenko et al., 2020). Like most, if not all, classical cadherins, however, the stability of N-cadherin is also p120 dependent. Thus, in the context of EMT-mediated metastatic dissemination, p120 ablation might conceivably impair early events in the metastatic cascade via destabilization of N-cadherin, and/or late events (e.g. MET and colonization) via destabilization of E-cadherin. Variations on this theme have been proposed for collective migration and the models are not necessarily mutually exclusive (Thiery et al., 1988; Wagner et al., 2007; Theveneau and Mayor, 2012; Peglion et al., 2014).

These observations are important because dysregulation of E-cadherin function and/or expression to varying degrees is evident in the vast majority of human cancer, 90% of which is epithelial in origin. The effects are generally interpreted in the obvious context of adhesion. However, our findings suggest that p120 and/or E-cadherin dysfunction may have other important consequences, including pro-metastatic conditioning of the tumor microenvironment, that are not yet fully appreciated. Moreover, this is not the first report of significant adverse consequences to the microenvironment associated with conditional p120 ablation. Although effects vary widely depending on the tissue, p120 ablation in the skin (Perez-Moreno et al., 2006) or the esophagus (Stairs et al., 2011) have significant inflammatory effects that appear to be causally linked to tumorigenesis. The possibility that such effects contribute significantly to the immune and microenvironmental conditions underlying tumorigenesis remains largely unexplored.

Though paradoxical at face value, our data are consistent with the notion of distinct roles for p120 at different stages of the metastatic cascade. In the mouse model used herein (MMTV-mT; MMTV-Cre; p120<sup>fl/fl</sup>), MMTV is activated around three weeks of age and controls both the tumor-initiating event (i.e. expression of mT) and the timing of p120 ablation (via upregulation of Cre), which occur more or less simultaneously. Thus, p120-ablation is, by definition, a very early event in this model that clearly increases both the number and size of p120-positive pulmonary metastatic lesions.

There are two general models relevant to the nature and timing of metastatic dissemination (Peglion et al., 2014; VanderVorst et al., 2019; Huang et al., 2015; Kota et al., 2019). The ‘linear’ progression model posits that metastasis-competent subclones arise late in tumor progression due to accumulation over time of genetic and epigenetic alterations. According to this model, metastases typically develop from aggressive late-stage subclones of the primary tumor and therefore share, at least initially, the same spectrum of genetic alterations. For example, if loss of p120 (or E-cadherin) were to trigger metastasis directly, one might expect this event to be reflected in the actual metastases, but that is not what we observed. p120-null cells were almost entirely excluded from metastatic lesions. This result is particularly striking in experiments where the early stages of metastasis are bypassed altogether by introducing the p120-null cells directly into the blood via tail vein injection.

In contrast, the ‘parallel’ progression model suggests that metastatic dissemination is an early event and that primary and metastatic clones



evolve independently thereafter. Loss of E-cadherin, for example, is typically viewed as a late event in tumor progression and a key mediator of the transition to metastasis. In our experiments, however, deletion of p120 was, by definition, an early event, and the metastatic lesions exacerbated by this event did not contain this mutation. Thus, we suggest that the early effects of p120 ablation with respect to successful metastatic colonization are not cell autonomous. Instead, the metastasis promoting effects of the p120-null cell pool appear to manifest indirectly at the level of the primary tumor, most likely functioning to accelerate dissemination of p120-expressing cells. Thereafter, retention of p120 becomes a major discriminating factor with respect to successful metastatic colonization.

We showed recently in Apc mouse models of intestinal cancer that loss of one p120 allele dramatically increases tumor multiplicity. Surprisingly, however, loss of the second allele did not further enhance tumorigenesis, but rather turned out to be synthetic lethal with loss of Apc. Thus, complete loss of p120 was never observed in these Apc-LOH-initiated tumors because intestinal stem cells exhibiting loss of both proteins were rapidly eliminated (Short et al., 2017, 2019). This phenomenon applies to both  $\alpha$ -catenin and E-cadherin, providing a compelling explanation for why complete loss of E-cadherin function is almost invariably a late event in intestinal cancer. These observations clearly imply the existence of a failsafe mechanism that somehow restricts complete loss of E-cadherin function during the early stages of intestinal tumor formation. Complete loss of E-cadherin function does, however, occur in late-stage tumors, suggesting that the failsafe mechanism(s) itself eventually fails as tumors progress to malignancy.

In closing, it is worth mentioning that retention of p120 (and E-cadherin) at distant metastatic sites was surprising, in part, because E-cadherin is widely viewed as a metastasis suppressor. By any conventional interpretation of the literature, one would expect metastases promoted by p120 ablation to be comprised largely, if not entirely, of p120-negative (E-cadherin-deficient) cells. Instead, our results reveal a strong selective pressure for p120 retention and are largely in line with a rapidly emerging literature on E-cadherin. In particular, it is increasingly clear that several modes of metastatic dissemination and/or colonization are dependent on the expression or re-expression of E-cadherin. One example is metastatic dissemination through collective migration (Huang et al., 2015; VanderVorst et al., 2019; Cheung and Ewald, 2016), a known p120- and E-cadherin-dependent process (Macpherson et al., 2007; Kota et al., 2019; Gritsenko et al., 2020). Remarkably, all of these dedicated metastatic processes are partly, if not wholly, dependent on the so-called ‘metastasis suppressor’ E-cadherin. Our data and conclusions, by and large, are in line with related evidence published recently by Ewald and colleagues for E-cadherin (Padmanaban et al., 2019).

## MATERIALS AND METHODS

### Patient cohort and tissue samples

A cohort of clinically characterized breast cancer patients with primary invasive ductal cancer diagnosed from 1991–2005 at the University Hospital Zurich was enrolled in the tissue microarray (TMA) study as described elsewhere (Theurillat et al., 2007). Informed consent was obtained for all tissue donors and all clinical investigations were conducted according to the principles expressed in the Declaration of Helsinki. Tumor grade was performed according to the modified Bloom and Richardson system (Bocker, 2002; Hanby and Walker, 2004). Of this cohort, invasive ductal carcinomas were studied. For clinicopathological parameters, see Table S1. Because 10% of the patients were followed-up >120 months, follow-up time was censored in all survival analyses presented in this article. The study was

approved by the ethical committee of the Kanton of Zurich (reference number StV-12-2005).

### Immunohistochemistry on patient samples

All antibodies were tested on a multi-tissue TMA for appropriate dilution and were used in a diagnostic protocol. Monoclonal antibodies (mAbs) against p120 (BD Bioscience, clone 98/pp120, 1:200), E-cadherin (Cell Marque Lifescreen Ltd., Rocklin, CA, USA, clone EP700Y, 1:200), Ki-67 (Dako, Glostrup, Denmark, clone MIB1, 1:20) and p63 [Thermo Scientific Lab Vision, Thermo Scientific, 4A4+Y4A3 (63P02), 1:200] were used. All immunohistochemical stains were performed on a Ventana Benchmark® platform (Ventana Medical Systems, Tucson, AZ). The CC1 standard pretreatment with 60 min boiling in pH 8 Tris-HCl buffer (Ventana) was followed by incubation with primary mAb (dilution 1:200) for 60 min at room temperature (RT) and development with the Ultraview-HRP kit (Ventana/Roche), including incubation with respective secondary antibody for 30 min at RT. Anti-p120 antibody was diluted in Tris containing 1% BSA. For counterstains, hematoxylin was used. p120 immunoreactivity at the tumor cell membrane was semi-quantitatively evaluated applying a four-tiered system (score 0, negative; score 1, weak discontinuous expression; score 2, moderate continuous expression; and score 3, strong continuous expression). Cytoplasmic p120 staining was scored as negative (score 0), weak (score 1), moderate (score 2) and strong (score 3). Scoring was done by three experienced pathologists (A.N., Z.V. and V.T) who were blind to sample identity until after data was recorded. Normal breast glands served as positive internal control and a standard for score 3. E-cadherin was evaluated at the tumor cell membrane as positive (strong expression) and negative (partial or complete loss of expression) cases (S. B.) Estrogen receptor status and HER2 FISH analysis were performed as described elsewhere (Theurillat et al., 2007).

### Animals

To generate mammary-specific p120 KO mice, p120<sup>f/f</sup> mice were backcrossed onto an FVB/NJ background and crossed with MMTV-cre#7 obtained from Dr William Muller (Department of Biochemistry, McGill University, Montreal, Canada) on an FVB background (Andrechek et al., 2000, 2005; Perez-Moreno et al., 2006; Kurley et al., 2012). p120 ablation in a mouse model of breast cancer was achieved by crossing the mammary-specific p120 KO mice with an FVB backcrossed version of MMTV-Polyoma Middle T (PyMT) model (Guy et al., 1992). All experiments involving animals were approved by the Vanderbilt University Institutional Animal Care and Use Committee.

### Immunohistochemistry and immunofluorescence on mouse samples

Fluorescent immunostaining on tissue was performed as previously described (Perez-Moreno et al., 2006; Kurley et al., 2012). Briefly, tissues were fixed in 10% formalin. Paraffin-embedded tissue sections were deparaffinized and rehydrated. Antigen retrieval was performed by boiling slides in 10 mM sodium citrate pH 6.0 for 10 min. After blocking, slides were incubated in primary and secondary antibody overnight and for 2 h, respectively. Primary antibodies against the following were utilized: p120 (F1 $\alpha$ SH, 0.8  $\mu$ g/ml), E-cadherin (0.5  $\mu$ g/ml, BD Biosciences),  $\beta$ -catenin (1:800, Sigma-Aldrich), keratin-8 (TROMA-I 1:1000, 0.2  $\mu$ g/ml, University of Iowa Hybridoma Core), F4/80 (1:200, AbDSerotec; requires trypsin antigen retrieval), SMA (0.2  $\mu$ g/ml, Sigma-Aldrich), Meca32 (1:100, BD Biosciences). Secondary antibodies (1:500, Invitrogen) were conjugated to Alexa Fluor 488, 594 or 647. Sections were mounted with Prolong Gold Antifade Mounting Medium (Invitrogen, Carlsbad, California, USA). Tissue processing, hematoxylin and eosin (H&E) staining, and immunohistochemistry for CD31 (1:100, Dianova) and CD3 (1:600, Santa Cruz Biotechnology) was performed by the Vanderbilt Translational Pathology Shared Resource Core. TUNEL staining assays were performed as per the manufacturer’s instructions with the following modification: antigen retrieval for 10 min in proteinase K (Millipore, Danvers, Massachusetts, USA). Staining was visualized using an Axioplan 2 microscope (Zeiss, Oberkochen, Germany). Images were collected with

either an Olympus QColor 3TM digital camera or a Hamamatsu Orca ER fluorescent camera and processed using MetaMorph software.

### Cell immunofluorescence

Cells were plated on glass coverslips and fixed in 3% paraformaldehyde for 30 min. After PBS washes, cells were permeabilized in PBS with 0.2% Triton X-100 for 5 min. After more PBS washes, non-specific binding was blocked using PBS with 3% non-fat milk. Cells were incubated in primary antibody for 30 min, washed, and incubated in secondary antibody for 30 min. After 3 PBS washes, nuclei were stained using Hoechst dye #33342. Coverslips were coated in ProLong gold (Invitrogen) and mounted on glass slides. Quantification of staining was assessed in  $n=6$  mice per genotype, in one section encompassing random pieces of tissue, and six images per section. When possible, p120-negative regions for KO animals were determined using co-immunofluorescence staining.

### Generation and manipulation of PyMT-derived cell lines

Tumor tissue was collected under sterile conditions, minced into 1 mm size pieces, and incubated in digest medium (DMEM/F12, with 1% antibiotic/antimycotic, 100 units/ml hyaluronidase, 3 mg/ml collagenase A and gentamycin) for 3–4 h with agitation at 37°C. Cells were pelleted in a Sorvall RT7 desktop centrifuge at 1000 RPM and washed five times in PBS supplemented with 5% adult bovine serum. Fibroblasts were removed by resuspending the pellet in low-serum medium (1% adult calf serum in DMEM/F12 medium) and plating the material on a sterile Petri dish. After 1 h in the incubator, cells not attached to the dish were spun down and resuspended in full growth medium (DMEM/F12, with 5% adult bovine serum, insulin, progesterone, 17 $\beta$ -estradiol, EGF, 1% antibiotic/antimycotic and gentamicin). Cells were plated onto collagen-coated plates and allowed to adhere for 48 h before changing of the medium. Cell lines were established by passaging cells at least 15 times prior to experimental use, after which point they were grown in DMEM supplemented with 10% FBS. To generate matched cell lines with and without p120, cell lines were transduced with lentiviral constructs expressing non-targeting shRNA (control) or Cre-recombinase (p120 KO) and then cells were selected for by puromycin treatment.

### Wound healing assays

PyMT-derived cells were plated to confluence and scratched with a P200 tip to generate the wound. Cells were rinsed with PBS, covered in growth medium, and imaged at six regions per scratch every 6 h. Images were acquired using an Axiovert 200 M microscope (Zeiss) and processed using MetaMorph software.

### Transwell invasion assays

Matrigel-coated transwells were equilibrated by the manufacturer's instructions. Cells were then plated in serum-free medium in the top well and promoted to invade toward 10% medium in the bottom chamber. After 24–48 h, transwells were fixed and stained using a Diff-Quik staining kit (Allegiance). Ten random fields of view per transwell were analyzed. For macrophage invasion assays, intraperitoneal injections with 2 ml thioglycolate were performed using a 27G needle. After 4 days, the abdominal cavity was filled with PBS, and peritoneal macrophages were isolated. Macrophages were pelleted and resuspended in serum-free medium and immediately used for invasion assays as described above. To generate the stimulus for macrophage invasion, PyMT-derived cells were grown in 3D Matrigel cultures for at least 7 days. Serum-free medium was added to the cultures, collected after 24 h and used for invasion induction of macrophages.

### Western blot analysis

Protein was isolated as previously described (Mariner et al., 2004). Briefly, cells were washed with PBS, lysed in RIPA buffer (50 mM Tris-HCl pH 7.4, 150 mM NaCl, 1% Nonidet P-40, 0.5% deoxycholic acid and 0.1% SDS) containing inhibitors (1 mM PMSF, 5  $\mu$ g/ml leupeptin, 2  $\mu$ g/ml aprotinin, 1 mM sodium orthovanadate, 1 mM EDTA, 50 mM NaF, 40 mM  $\beta$ -glycerophosphate) and spun at 14,000  $g$  at 4°C for 5 min. Cleared total protein was quantified using a bicinchoninic acid assay (Pierce, Rockford, IL). 20  $\mu$ g of protein per sample were boiled in 2 $\times$  Laemmli sample buffer and

separated by SDS-PAGE electrophoresis. Proteins were transferred to nitrocellulose (PerkinElmer, Waltham, MA). Non-specific binding was blocked by incubating membranes in 3% non-fat milk in Tris-buffered saline and Odyssey blocking buffer (LI-COR, Lincoln, NE) prior to the addition of primary and secondary antibodies, respectively. Anti-p120 (mAb pp120, 0.1  $\mu$ g/ml, BD Biosciences), anti-E-cadherin (0.1  $\mu$ g/ml, BD Biosciences), anti-tubulin/DM1 $\alpha$  (1:1000, Sigma-Aldrich), anti-N-cadherin (0.8  $\mu$ g/ml 13A9, Millipore), and anti-P-cadherin (1:250, BD Biosciences) antibodies were used (cat. numbers are provided in immunohistochemistry section). The Odyssey system was used for the detection of secondary goat anti-mouse-IgG IRDye 800CW antibodies (1:10,000, LI-COR).

### Orthotopic transplant

$10^6$  cells were suspended in 50  $\mu$ l of 1:1 type I collagen (1.19 mg/ml final concentration) to neutralization solution (100 mM Hepes in 2 $\times$  PBS, pH 7.3). Plugs were allowed to solidify for 1 h in the incubator and then covered in growth medium. The following day plugs were transplanted into the cleared fat mammary fat pads of 3-week-old female mice. Tumor growth was assessed by caliper and tumors and lungs were collected 5 weeks after transplant.

### Tail vein injections and lung whole mount

PyMT-derived cells were trypsinized, pelleted and washed three times in PBS. After passage through a 70  $\mu$ m strainer,  $10^6$  cells per 100  $\mu$ l were injected into the tail vein of mice. After 4 weeks, mice were killed, and lungs were collected. Lungs were analyzed by whole-mount and tumor burden analysis. Tumor burden was quantified as the percentage of metastases area to total lung area at three depths per lung. For lung whole mount, lungs were inflated with formalin and fixed overnight. Lungs were then dehydrated in progressive increasing amounts of ethanol and cleared overnight in Histoclear. Rehydration the next day was followed by staining in Mayer's hematoxylin. After destain steps in 1% HCl solution and water, lungs were dehydrated and cleared once again. Analysis of lung metastases was performed using a dissecting scope and an Olympus QColor 3TM digital camera.

### Whole tumor

Tumors were collected, minced and incubated in digest medium (RPMI with 1 mg/ml collagenase I and 1 mg/ml dispase II) for 2 h at 37°C. Tumor material was then pressed through a 70  $\mu$ m cell strainer in 10 ml cold PBS and repeated for a total of 50 ml PBS. Tumor cells were then treated with 10  $\mu$ l of 5MU/ml DNaseI for 5 min at room temperature. Cells were pelleted at 300  $g$  to remove DNase. Red blood cells were removed from tumor preparations using lysis buffer. Cells were washed with PBS, strained, and then counted in the presence of Trypan Blue. Each sample of  $5 \times 10^6$  cells per 100  $\mu$ l flow buffer (PBS, 0.5% BSA and 2 mM EDTA) was treated with Fc block and incubated with fluorophore-conjugated antibodies for 30 min on ice. All antibodies for flow cytometry were purchased through eBioscience. To detect M1-macrophages, fluor-conjugated monoclonal antibodies to CD80 (16-10A1) and CD86 (25-0862) were used at 0.5  $\mu$ g/ml. M2-macrophages were detected with fluor-conjugated monoclonal antibodies to CD206 (53-2069-42) and CD204 (25-2046-82) at a concentration of 1  $\mu$ g per ml. After 2 washes with flow buffer, cells were analyzed by flow cytometry by the Vanderbilt Flow Cytometry Shared Resource Core.

### Anchorage independent and 3D Matrigel growth

For anchorage-independent growth assays, 6-well dishes were coated with a layer of 0.7% low gelling temperature agarose.  $5 \times 10^3$  PyMT-derived cells suspended in 0.35% agarose were plated per well and covered in 2 ml growth medium. After 3.5 weeks of growth, colonies were imaged using an inverted microscope. For 3D growth assays, 35 mm tissue culture dishes were coated with 500  $\mu$ l of Matrigel.  $7 \times 10^5$  PyMT-derived cells were plated in growth medium supplemented with 2% Matrigel.

### qRT-PCR on macrophages

Total RNA was extracted from sorted CD45<sup>+</sup> CD11b<sup>+</sup> F4/80<sup>+</sup> cells from tumors of d54 PyMT control and p120 KO mice ( $n=3$  per genotype) using

QIAshredder columns and an RNeasy mini kit (Qiagen). cDNA was synthesized using Invitrogen Superscript Firststrand synthesis system for RT-PCR (Invitrogen). Primers specific for iNOS, TNF $\alpha$ , IL-12, IL-6, IL-1b, VEGF, MMP2, MMP9, MMP13, CXCL1 and IL-10 were used (sequence of primers are available upon request) and the relative gene expression was determined using ABI PRISM 7900HT Sequence Detection System (PE Applied Biosystems). The comparative threshold cycle method was used to calculate gene expression normalized to  $\beta$ -actin expression.

### Circulating tumor cell assays

At 54 days after initial palpation mice were euthanized ( $n=4$  per genotype) and whole blood was collected in a heparinized needle. Each well of a six-well dish was coated in 1:1 mix of Matrigel and DMEM supplemented with 10% FBS. After Matrigel solidification, 500  $\mu$ l of whole blood was plated per 6-well dish and covered in 2 ml DMEM. After 48 h, cultures were washed with PBS. Red blood cells were removed with lysis buffer (155 mM NH $_4$ Cl, 12 mM NaHCO $_3$  and 0.1 mM EDTA) and then washed away with PBS. Colonies were then allowed to grow for 7–10 days with medium changes every 3–4 days. Colonies were counted in five random 2.5 $\times$  fields and 10 random 10 $\times$  fields. For qRT-PCR experiments, RNA was isolated from whole blood and qRT-PCR assays conducted were performed as previously described (Connelly et al., 2011).

### Statistical analysis

Statistical analyses for non-clinical data were performed using GraphPad Prism (GraphPad La Jolla, CA) as described in figure legends. For assays with or without normal distribution, two-tailed Student's  $t$ -tests or Mann–Whitney tests were performed, respectively. For clinical samples, associations of staining intensity with clinicopathological parameters were undertaken by descriptive statistics [cross tables, two-tailed Fisher's exact test, and two-tailed  $\chi^2$  test for trends (linear-by-linear)]. For correlation significance between immunohistochemical and fluorescence *in-situ* based markers, Kendall's tau  $b$  for non-parametric correlations was used.  $P<0.05$  was considered significant. Correlations of p120 expression with overall survival were calculated.

### Acknowledgements

We are grateful to members of the Reynolds laboratory, Dr Carlos L. Arteaga and laboratory, Dr David Vaught, and Dr Andrew Smith for helpful discussions of this work. We would like to acknowledge Martina Storz, Susanne Detwiler and Jasmin Roth for their excellent technical assistance. Some of the text and figures in this paper formed part of Sarah Jean Kurley's PhD thesis in the Department of Cancer Biology at Vanderbilt University in 2012.

### Competing interests

The authors declare no competing or financial interests.

### Author contributions

Conceptualization: S.J.K., V.T., B.B., S.V.N., R.H.C., A.B.R.; Methodology: S.J.K., V.T., S.V.N., R.S.C., W.J.M., A.B.R.; Validation: V.T., B.B., A.N., Z.V., S.B.; Formal analysis: S.J.K., V.T., S.V.N., R.H.C., R.S.C., A.B.R.; Investigation: S.J.K., V.T., B.B., A.N., Z.V., U.Z.-H., R.H.C., A.B.R.; Resources: S.V.N., A.N., Z.V., U.Z.-H., R.S.C., W.J.M., A.B.R.; Data curation: A.N., Z.V., S.B.; Writing - original draft: S.J.K., A.B.R.; Writing - review & editing: S.J.K., B.B., U.Z.-H., S.B., R.H.C., R.S.C., W.J.M., A.R., A.B.R.; Visualization: A.B.R.; Supervision: R.H.C., A.B.R.; Project administration: A.B.R.; Funding acquisition: A.B.R.

### Funding

Technical support was provided by the following Vanderbilt University Core Resources: VUMC Cell Imaging Shared Resource (CA68485, DK20593, DK58404, HD15052, DK59637 and EY08126); Translational Pathology Shared Resource; and VMC Flow Cytometry Shared Resource (P30 CA68485, DK058404). This work was supported by the National Institutes of Health (NIH) grants R01 CA111947 and R01 CA55724 to A.B.R., 2PO1CA099031-06A1 to W.J.M., and Predoctoral Trainee Award BC083306 to S.J.K. Funding was also received through the Vanderbilt Cancer Center Support Grant (NIH, P30 CA068485) and a Pilot Grant to A.B.R. through the Vanderbilt Breast SPOR (NIH; P50 CA98131). Deposited in PMC for release after 12 months.

### Supplementary information

Supplementary information available online at <https://jcs.biologists.org/lookup/doi/10.1242/jcs.250639.supplemental>

### References

- Andrechek, E. R., Hardy, W. R., Siegel, P. M., Rudnicki, M. A., Cardiff, R. D. and Muller, W. J. (2000). Amplification of the neu/erbB-2 oncogene in a mouse model of mammary tumorigenesis. *Proc. Natl. Acad. Sci. USA* **97**, 3444–3449. doi:10.1073/pnas.97.7.3444
- Andrechek, E. R., White, D. and Muller, W. J. (2005). Targeted disruption of ErbB2/Neu in the mammary epithelium results in impaired ductal outgrowth. *Oncogene* **24**, 932–937. doi:10.1038/sj.onc.1208230
- Berx, G., Cleton-Jansen, A. M., Nollet, F., de Leeuw, W. J., van de Vijver, M., Cornelisse, C. and van Roy, F. (1995). E-cadherin is a tumour/invasion suppressor gene mutated in human lobular breast cancers. *EMBO J.* **14**, 6107–6115. doi:10.1002/j.1460-2075.1995.tb00301.x
- Bocker, W. (2002). [WHO classification of breast tumors and tumors of the female genital organs: pathology and genetics]. *Verh. Dtsch. Ges. Pathol.* **86**, 116–119.
- Brabletz, T. (2012). EMT and MET in metastasis: where are the cancer stem cells? *Cancer Cell* **22**, 699–701. doi:10.1016/j.ccr.2012.11.009
- Chetty, R. and Serra, S. (2008). Nuclear E-cadherin immunoexpression: from biology to potential applications in diagnostic pathology. *Adv. Anat. Pathol.* **15**, 234–240. doi:10.1097/PAP.0b013e31817bf566
- Cheung, K. J. and Ewald, A. J. (2016). A collective route to metastasis: seeding by tumor cell clusters. *Science* **352**, 167–169. doi:10.1126/science.aaf6546
- Connelly, L., Barham, W., Onishko, H. M., Sherrill, T., Chodosh, L. A., Blackwell, T. S. and Yull, F. E. (2011). Inhibition of NF-kappa B activity in mammary epithelium increases tumor latency and decreases tumor burden. *Oncogene* **30**, 1402–1412. doi:10.1038/onc.2010.521
- Davis, M. A. and Reynolds, A. B. (2006). Blocked acinar development, E-cadherin reduction, and intraepithelial neoplasia upon ablation of p120–catenin in the mouse salivary gland. *Dev. Cell* **10**, 21–31. doi:10.1016/j.devcel.2005.12.004
- DeNardo, D. G. and Coussens, L. M. (2007). Inflammation and breast cancer. Balancing immune response: crosstalk between adaptive and innate immune cells during breast cancer progression. *Breast Cancer Res.* **9**, 212. doi:10.1186/bcr1746
- Derksen, P. W., Braumuller, T. M., van der Burg, E., Hornsveld, M., Mesman, E., Wesseling, J., Krimpenfort, P. and Jonkers, J. (2011). Mammary-specific inactivation of E-cadherin and p53 impairs functional gland development and leads to pleomorphic invasive lobular carcinoma in mice. *Dis. Model. Mech.* **4**, 347–358. doi:10.1242/dmm.006395
- Dillon, D. A., D'Aquila, T., Reynolds, A. B., Fearon, E. R. and Rimm, D. L. (1998). The expression of p120<sup>cas</sup> protein in breast cancer is independent of alpha- and beta-catenin and E-cadherin. *Am. J. Pathol.* **152**, 75–82.
- El Sharouni, M.-A., Postma, L. and van Diest, P. J. (2017). Correlation between E-cadherin and p120 expression in invasive ductal breast cancer with a lobular component and MRI findings. *Virchows Arch.* **471**, 707–712. doi:10.1007/s00428-017-2203-2
- Fan, X., Jin, S., Li, Y., Khadaroo, P. A., Dai, Y., He, L., Zhou, D. and Lin, H. (2019). Genetic and epigenetic regulation of E-cadherin signaling in human hepatocellular carcinoma. *Cancer Manag Res.* **11**, 8947–8963. doi:10.2147/CMAR.S225606
- Gritsenko, P. G., Atlasy, N., Dieteren, C. E. J., Navis, A. C., Venhuizen, J. H., Veelken, C., Schubert, D., Acker-Palmer, A., Westerman, B. A., Wurdinger, T. et al. (2020). p120-catenin-dependent collective brain infiltration by glioma cell networks. *Nat. Cell Biol.* **22**, 97–107. doi:10.1038/s41556-019-0443-x
- Gunasinghe, N. P. A., Wells, A., Thompson, E. W. and Hugo, H. J. (2012). Mesenchymal-epithelial transition (MET) as a mechanism for metastatic colonisation in breast cancer. *Cancer Metastasis Rev.* **31**, 469–478. doi:10.1007/s10555-012-9377-5
- Guy, C. T., Cardiff, R. D. and Muller, W. J. (1992). Induction of mammary tumors by expression of polyomavirus middle T oncogene: a transgenic mouse model for metastatic disease. *Mol. Cell. Biol.* **12**, 954–961. doi:10.1128/MCB.12.3.954
- Hanby, A. M. and Walker, C. (2004). The WHO, and what of the breast and female genital organs: part IV in the WHO classification of tumours series. *Breast Cancer Res.* **6**, 133–134. doi:10.1186/bcr788
- Hendley, A. M., Wang, Y. J., Polireddy, K., Alsina, J., Ahmed, I., Lafaro, K. J., Zhang, H., Roy, N., Savidge, S. G., Cao, Y. et al. (2016). p120 Catenin suppresses basal epithelial cell extrusion in invasive pancreatic neoplasia. *Cancer Res.* **76**, 3351–3363. doi:10.1158/0008-5472.CAN-15-2268
- Hernández-Martínez, R., Ramkumar, N. and Anderson, K. V. (2019). p120-catenin regulates WNT signaling and EMT in the mouse embryo. *Proc. Natl. Acad. Sci. USA* **116**, 16872–16881. doi:10.1073/pnas.1902843116
- Hu, G. (2012). p120-Catenin: a novel regulator of innate immunity and inflammation. *Crit. Rev. Immunol.* **32**, 127–138. doi:10.1615/CritRevImmunol.v32.i2.20
- Huang, B., Jolly, M. K., Lu, M., Tsarfaty, I., Ben-Jacob, E. and Onuchic, J. N. (2015). Modeling the transitions between collective and solitary migration phenotypes in cancer metastasis. *Sci. Rep.* **5**, 17379. doi:10.1038/srep17379

- Jeanes, A., Gottardi, C. J. and Yap, A. S. (2008). Cadherins and cancer: how does cadherin dysfunction promote tumor progression? *Oncogene* **27**, 6920-6929. doi:10.1038/onc.2008.343
- Jones, J., Wang, H., Karanam, B., Theodore, S., Dean-Colomb, W., Welch, D. R., Grizzle, W. and Yates, C. (2014). Nuclear localization of Kaiso promotes the poorly differentiated phenotype and EMT in infiltrating ductal carcinomas. *Clin. Exp. Metastasis* **31**, 497-510. doi:10.1007/s10585-014-9644-7
- Kang, Y. and Pantel, K. (2013). Tumor cell dissemination: emerging biological insights from animal models and cancer patients. *Cancer Cell* **23**, 573-581. doi:10.1016/j.ccr.2013.04.017
- Kim, S. A., Tai, C.-Y., Mok, L.-P., Mosser, E. A. and Schuman, E. M. (2011). Calcium-dependent dynamics of cadherin interactions at cell-cell junctions. *Proc. Natl. Acad. Sci. USA* **108**, 9857-9862. doi:10.1073/pnas.1019003108
- Kota, P., Terrell, E. M., Ritt, D. A., Insinna, C., Westlake, C. J. and Morrison, D. K. (2019). M-Ras/Shoc2 signaling modulates E-cadherin turnover and cell-cell adhesion during collective cell migration. *Proc. Natl. Acad. Sci. USA* **116**, 3536-3545. doi:10.1073/pnas.1805919116
- Kurley, S. J., Bierie, B., Carnahan, R. H., Lobdell, N. A., Davis, M. A., Hofmann, I., Moses, H. L., Muller, W. J. and Reynolds, A. B. (2012). p120-catenin is essential for terminal end bud function and mammary morphogenesis. *Development* **139**, 1754-1764. doi:10.1242/dev.072769
- Lin, E. Y., Jones, J. G., Li, P., Zhu, L., Whitney, K. D., Muller, W. J. and Pollard, J. W. (2003). Progression to malignancy in the polyoma middle T oncoprotein mouse breast cancer model provides a reliable model for human diseases. *Am. J. Pathol.* **163**, 2113-2126. doi:10.1016/S0002-9440(10)63568-7
- Macpherson, I. R., Hooper, S., Serrels, A., McGarry, L., Ozanne, B. W., Harrington, K., Frame, M. C., Sahai, E. and Brunton, V. G. (2007). p120-catenin is required for the collective invasion of squamous cell carcinoma cells via a phosphorylation-independent mechanism. *Oncogene* **26**, 5214-5228. doi:10.1038/sj.onc.1210334
- Mariner, D. J., Davis, M. A. and Reynolds, A. B. (2004). EGFR signaling to p120-catenin through phosphorylation at Y228. *J. Cell Sci.* **117**, 1339-1350. doi:10.1242/jcs.01001
- Mastracci, T. L., Tjan, S., Bane, A. L., O'Malley, F. P. and Andrusis, I. L. (2005). E-cadherin alterations in atypical lobular hyperplasia and lobular carcinoma in situ of the breast. *Mod. Pathol.* **18**, 741-751. doi:10.1038/modpathol.3800362
- Muraoka, R. S., Lenferink, A. E., Law, B., Hamilton, E., Brantley, D. M., Roebuck, L. R. and Arteaga, C. L. (2002). ErbB2/Neu-induced, cyclin D1-dependent transformation is accelerated in p27-haploinsufficient mammary epithelial cells but impaired in p27-null cells. *Mol. Cell. Biol.* **22**, 2204-2219. doi:10.1128/MCB.22.7.2204-2219.2002
- Nakopoulou, L., Gakiopoulou-Givalou, H., Karayiannakis, A. J., Giannopoulou, I., Keramopoulos, A., Davaris, P. and Pignatelli, M. (2002). Abnormal alpha-catenin expression in invasive breast cancer correlates with poor patient survival. *Histopathology* **40**, 536-546. doi:10.1046/j.1365-2559.2002.01392.x
- Oas, R. G., Xiao, K., Summers, S., Wittich, K. B., Chiasson, C. M., Martin, W. D., Grossniklaus, H. E., Vincent, P. A., Reynolds, A. B. and Kowalczyk, A. P. (2010). p120-Catenin is required for mouse vascular development. *Circ. Res.* **106**, 941-951. doi:10.1161/CIRCRESAHA.109.207753
- Ozawa, M. (2003). p120-independent modulation of E-cadherin adhesion activity by the membrane-proximal region of the cytoplasmic domain. *J. Biol. Chem.* **278**, 46014-46020. doi:10.1074/jbc.M307778200
- Padmanaban, B., Krol, L., Suhail, Y., Szczerba, B. M., Aceto, N., Bader, J. S., Ewald, A. J. (2019). E-cadherin is required for metastasis in multiple models of breast cancer. (2019). *Nature* **573**, 439-444. doi:10.1038/s41586-019-1526-3
- Peglion, F., Lense, F. and Etienne-Manneville, S. (2014). Adherens junction treadmill during collective migration. *Nat. Cell Biol.* **16**, 639-651. doi:10.1038/ncb2985
- Perez-Moreno, M., Davis, M. A., Wong, E., Pasolli, H. A., Reynolds, A. B. and Fuchs, E. (2006). p120-catenin mediates inflammatory responses in the skin. *Cell* **124**, 631-644. doi:10.1016/j.cell.2005.11.043
- Perez-Moreno, M., Song, W., Pasolli, H. A., Williams, S. E. and Fuchs, E. (2008). Loss of p120 catenin and links to mitotic alterations, inflammation, and skin cancer. *Proc. Natl. Acad. Sci. USA* **105**, 15399-15404. doi:10.1073/pnas.0807301105
- Reichert, M., Bakir, B., Moreira, L., Pitarresi, J. R., Feldmann, K., Simon, L., Suzuki, K., Maddipati, R., Rhim, A. D., Schlitter, A. M. et al. (2018). Regulation of epithelial plasticity determines metastatic organotropism in pancreatic cancer. *Dev. Cell* **45**, 696-711.e8. doi:10.1016/j.devcel.2018.05.025
- Richert, M. M., Phadke, P. A., Matters, G., DiGirolamo, D. J., Washington, S., Demers, L. M., Bond, J. S., Manni, A. and Welch, D. R. (2005). Metastasis of hormone-independent breast cancer to lung and bone is decreased by  $\alpha$ -difluoromethylornithine treatment. *Breast Cancer Res.* **7**, R819-R827. doi:10.1186/bcr1292
- Saijo, Y., Sato, G., Usui, K., Sato, M., Sagawa, M., Kondo, T., Minami, Y. and Nukiwa, T. (2001). Expression of nucleolar protein p120 predicts poor prognosis in patients with stage I lung adenocarcinoma. *Ann. Oncol.* **12**, 1121-1125. doi:10.1023/A:1011617707999
- Sarrió, D., Pérez-Mies, B., Hardisson, D., Moreno-Bueno, G., Suárez, A., Cano, A., Martín-Pérez, J., Gamallo, C. and Palacios, J. (2004). Cytoplasmic localization of p120ctn and E-cadherin loss characterize lobular breast carcinoma from preinvasive to metastatic lesions. *Oncogene* **23**, 3272-3283. doi:10.1038/sj.onc.1207439
- Schackmann, R. C., van Amersfoort, M., Haarhuis, J. H., Vlugg, E. J., Halim, V. A., Roodhart, J. M., Vermaat, J. S., Voest, E. E., van der Groep, P., van Diest, P. J. et al. (2011). Cytosolic p120-catenin regulates growth of metastatic lobular carcinoma through Rock1-mediated anoikis resistance. *J. Clin. Invest.* **121**, 3176-3188. doi:10.1172/JCI41695
- Schackmann, R. C. J., Klarenbeek, S., Vlugg, E. J., Stelloo, S., van Amersfoort, M., Tenhagen, M., Braumuller, T. M., Vermeulen, J. F., van der Groep, P., Peeters, T. et al. (2013a). Loss of p120-catenin induces metastatic progression of breast cancer by inducing anoikis resistance and augmenting growth factor receptor signaling. *Cancer Res.* **73**, 4937-4949. doi:10.1158/0008-5472.CAN-13-0180
- Schackmann, R. C. J., Tenhagen, M., van de Ven, R. A. H. and Derksen, P. W. B. (2013b). p120-catenin in cancer - mechanisms, models and opportunities for intervention. *J. Cell Sci.* **126**, 3515-3525. doi:10.1242/jcs.134411
- Short, S. P., Kondo, J., Smalley-Freed, W. G., Takeda, H., Dohn, M. R., Powell, A. E., Carnahan, R. H., Washington, M. K., Tripathi, M., Payne, D. M. et al. (2017). p120-Catenin is an obligate haploinsufficient tumor suppressor in intestinal neoplasia. *J. Clin. Invest.* **127**, 4462-4476. doi:10.1172/JCI77217
- Short, S. P., Barrett, C. W., Stengel, K. R., Revetta, F. L., Choksi, Y. A., Coburn, L. A., Lintel, M. K., McDonough, E. M., Washington, M. K., Wilson, K. T. et al. (2019). Kaiso is required for MTG16-dependent effects on colitis-associated carcinoma. *Oncogene* **38**, 5091-5106. doi:10.1038/s41388-019-0777-7
- Silvera, D. and Schneider, R. J. (2009). Inflammatory breast cancer cells are constitutively adapted to hypoxia. *Cell Cycle* **8**, 3091-3096. doi:10.4161/cc.8.19.9637
- Silvera, D., Arju, R., Darvishian, F., Levine, P. H., Zolfaghari, L., Goldberg, J., Hochman, T., Formenti, S. C. and Schneider, R. J. (2009). Essential role for eIF4G1 overexpression in the pathogenesis of inflammatory breast cancer. *Nat. Cell Biol.* **11**, 903-908. doi:10.1038/ncb1900
- Singhai, R., Patil, V. W., Jaiswal, S. R., Patil, S. D., Tayade, M. B. and Patil, A. V. (2011). E-Cadherin as a diagnostic biomarker in breast cancer. *N. Am. J. Med. Sci.* **3**, 227-233. doi:10.4297/najms.2011.3227
- Smalley-Freed, W. G., Efimov, A., Burnett, P. E., Short, S. P., Davis, M. A., Gumucio, D. L., Washington, M. K., Coffey, R. J. and Reynolds, A. B. (2010). p120-catenin is essential for maintenance of barrier function and intestinal homeostasis in mice. *J. Clin. Invest.* **120**, 1824-1835. doi:10.1172/JCI41414
- Smalley-Freed, W. G., Efimov, A., Short, S. P., Jia, P., Zhao, Z., Washington, M. K., Robine, S., Coffey, R. J. and Reynolds, A. B. (2011). Adenoma formation following limited ablation of p120-catenin in the mouse intestine. *PLoS ONE* **6**, e19880. doi:10.1371/journal.pone.0019880
- Stairs, D. B., Bayne, L. J., Rhoades, B., Vega, M. E., Waldron, T. J., Kalabis, J., Klein-Szanto, A., Lee, J. S., Katz, J. P., Diehl, J. A. et al. (2011). Deletion of p120-catenin results in a tumor microenvironment with inflammation and cancer that establishes it as a tumor suppressor gene. *Cancer Cell* **19**, 470-483. doi:10.1016/j.ccr.2011.02.007
- Sun, Y., Zhang, J. and Ma, L. (2014).  $\alpha$ -catenin. A tumor suppressor beyond adherens junctions. *Cell Cycle* **13**, 2334-2339. doi:10.4161/cc.29765
- Talvinen, K., Tuikkala, J., Nykänen, M., Nieminen, A., Anttinen, J., Nevalainen, O. S., Hurme, S., Kuopio, T. and Kronqvist, P. (2010). Altered expression of p120catenin predicts poor outcome in invasive breast cancer. *J. Cancer Res. Clin. Oncol.* **136**, 1377-1387. doi:10.1007/s00432-010-0789-8
- Theurillat, J. P., Ingold, F., Frei, C., Zippelius, A., Varga, Z., Seifert, B., Chen, Y.-T., Jäger, D., Knuth, A. and Moch, H. (2007). NY-ESO-1 protein expression in primary breast carcinoma and metastases: correlation with CD8+ T-cell and CD79a+ plasmacytic/B-cell infiltration. *Int. J. Cancer* **120**, 2411-2417. doi:10.1002/ijc.22376
- Theveneau, E. and Mayor, R. (2012). Cadherins in collective cell migration of mesenchymal cells. *Curr. Opin. Cell Biol.* **24**, 677-684. doi:10.1016/j.cob.2012.08.002
- Thiery, J. P., Boyer, B., Tucker, G., Gavrilovic, J. and Valles, A. M. (1988). Adhesion mechanisms in embryogenesis and in cancer invasion and metastasis. *Ciba Found Symp.* **141**, 48-74.
- Thoreson, M. A., Anastasiadis, P. Z., Daniel, J. M., Ireton, R. C., Wheelock, M. J., Johnson, K. R., Hummingbird, D. K. and Reynolds, A. B. (2000). Selective uncoupling of p120ctn from E-cadherin disrupts strong adhesion. *J. Cell Biol.* **148**, 189-202. doi:10.1083/jcb.148.1.189
- Valastyan, S. and Weinberg, R. A. (2011). Tumor metastasis: molecular insights and evolving paradigms. *Cell* **147**, 275-292. doi:10.1016/j.cell.2011.09.024
- VanderVorst, K., Dreyer, C. A., Konopelski, S. E., Lee, H., Ho, H.-H. and Carraway, K. L., III (2019). Wnt/PCP signaling contribution to carcinoma collective cell migration and metastasis. *Cancer Res.* **79**, 1719-1729. doi:10.1158/0008-5472.CAN-18-2757
- Vos, C. B., Cleton-Jansen, A. M., Bex, G., de Leeuw, W. J., ter Haar, N. T., van Roy, F., Cornelisse, C. J., Peterse, J. L. and van de Vijver, M. J. (1997). E-cadherin inactivation in lobular carcinoma in situ of the breast: an early event in tumorigenesis. *Br. J. Cancer* **76**, 1131-1133. doi:10.1038/bjc.1997.523

- Wagner, W., Roderburg, C., Wein, F., Diehlmann, A., Frankhauser, M., Schubert, R., Eckstein, V. and Ho, A. D.** (2007). Molecular and secretory profiles of human mesenchymal stromal cells and their abilities to maintain primitive hematopoietic progenitors. *Stem Cells* **25**, 2638-2647. doi:10.1634/stemcells.2007-0280
- Wehrendt, D. P., Carmona, F., González Wusener, A. E., González, A., Martínez, J. M. L. and Arregui, C. O.** (2016). P120-Catenin regulates early trafficking stages of the N-cadherin precursor complex. *PLoS ONE* **11**, e0156758. doi:10.1371/journal.pone.0156758
- Wells, A., Yates, C. and Shepard, C. R.** (2008). E-cadherin as an indicator of mesenchymal to epithelial reverting transitions during the metastatic seeding of disseminated carcinomas. *Clin. Exp. Metastasis* **25**, 621-628. doi:10.1007/s10585-008-9167-1
- Wijnhoven, B. P., Pignatelli, M., Dinjens, W. N. and Tilanus, H. W.** (2005). Reduced p120ctn expression correlates with poor survival in patients with adenocarcinoma of the gastroesophageal junction. *J. Surg. Oncol.* **92**, 116-123. doi:10.1002/jso.20344